

# Study of Heat Transfer in the Absorber Plates of a Flat-Plate Solar Collector Using Dual-Phase-Lag Model

Yu-Ching Yang, Haw-Long Lee, Win-Jin Chang

**Abstract**—The present work numerically analyzes the transient heat transfer in the absorber plates of a flat-plate solar collector based on the dual-phase-lag (DPL) heat conduction model. An efficient numerical scheme involving the hybrid application of the Laplace transform and control volume methods is used to solve the linear hyperbolic heat conduction equation. This work also examines the effect of different medium parameters on the behavior of heat transfer. Results show that, while the heat-flux phase lag induces thermal waves in the medium, the temperature-gradient phase lag smoothens the thermal waves by promoting non-Fourier diffusion-like conduction into the medium.

**Keywords**—Absorber plates, dual-phase-lag, non-Fourier, solar collector.

## I. INTRODUCTION

SOLAR collectors are special kinds of heat exchangers that transform solar radiating energy to internal energy of the transport medium. Among the various types of collectors, flat-plate collectors are the common choices for this conversion, probably due to its simple design and ease of fabrication. A flat-plate solar collector is a device, which absorbs the incoming solar radiation, converts it into heat, and then transfers this heat to a fluid flowing through the tubes. This device has found its wide applications in space heating and cooling, solar refrigeration systems, solar thermal systems, industrial process heating, etc. [1]. Among the various components of a flat-plate solar collector, the absorber plate is the main accountable for the conversion of solar energy into thermal energy. Therefore, the thermal performance of a flat-plate collector is strongly influenced by the performance of the absorber plate.

The well-known DPL heat conduction model, proposed by Tzou [2], [3], introduces the phase lags of temperature gradient and heat flux to account for the microstructural interactions in the fast, transient process of heat transport and it takes the form:

$$q(r, t + \tau_q) = -k\nabla T(r, t + \tau_T)$$

where  $\tau_T$  is the phase lag of the temperature gradient. The phase lag  $\tau_T$  is interpreted as the time delay caused by the

Yu-Ching Yang is with Kun Shan University, Tainan, Taiwan, ROC (corresponding author, phone: 886-6-2050496; fax: 886-6-2050509; e-mail: ycyang@mail.ksu.edu.tw).

Haw-Long Lee and Win-Jin Chang are with Kun Shan University, Tainan, Taiwan, ROC (e-mail: changwj@mail.ksu.edu.tw, hawlong@mail.ksu.edu.tw).

microstructural interactions such as phonon–electron interactions or phonon scattering, while the phase lag  $\tau_q$  can be interpreted as the relaxation time due to the fast transient effects of thermal inertia. Ever since its agreement with experimental results was demonstrated [3], the DPL model has attracted a considerable interest in a wide variety of scientific and engineering fields. For example, Hu and Chen [4] solved the transient temperature field around a partially insulated crack in a half-plane by applying DPL heat conduction model. Lee et al. [5] numerically investigated the transient heat transfer in a thin metal film exposed to short-pulse laser heating. Liu and Wang [6] analyzed the thermal response for estimating thermal damage in laser-irradiated biological tissue. Recently, Afrin et al. [7] analytically investigated the heat conduction in a gas-saturated porous medium subjected to a short-pulsed laser heating.

Recently, Kundu and Lee [8] presented an analytical study of non-Fourier heat conduction for the absorber plates of a flat-plate solar collector. They concluded that not considering non-Fourier heat transfer of the absorber plate may not be a wise decision under certain design conditions. To accommodate the microstructural effect, the present work further applies DPL heat conduction model to explore the transient heat transfer in the absorber plates of a flat-plate solar collector. The problem is solved numerically and, to the best of the authors' knowledge, it is the first time in the literature to study such a problem based on the DPL heat conduction model.

## II. ANALYSIS

### A. Physical Model and Mathematical Formulation

The main components of a flat-plate solar collector are the absorber plate and fluid carrying tubes. The arrangement of the absorber plate and fluid carrying tubes is shown in Fig. 1. For the thermal analysis of an absorber plate, a symmetric heat transfer module which acts as a fin subject to the insulated tip and a constant base temperature is taken. On the assumption that  $t_p/L=1$ , the one-dimensional energy equation for the absorber plate in a flat-plate collector shown in Fig. 1 can be written as [8]:

$$-\frac{\partial q(x, t)}{\partial x} - \frac{2h}{t_p}(T - T_a) + \frac{g}{t_p} = \rho c \frac{\partial T(x, t)}{\partial t} \quad (1)$$

where  $h$  is the convection heat transfer coefficient and  $g$  is the

absorbed solar radiation which is an instantaneous value taken for the development of the solution. In reality, it may change with time.

The one-dimensional DPL constitutive equation for the absorber plate can be expressed as [9]:

$$q(x,t) + \tau_q \frac{\partial q(x,t)}{\partial t} = -k \frac{\partial T(x,t)}{\partial x} - k \tau_T \frac{\partial^2 T(x,t)}{\partial t \partial x} \quad (2)$$

Elimination  $q(x,t)$  from (1) and (2) yields the following hyperbolic heat conduction equation of this problem as:

$$\tau_q \rho c \frac{\partial^2 T}{\partial t^2} + \rho c \frac{\partial T}{\partial t} = k \frac{\partial^2}{\partial x^2} [\tau_T \frac{\partial T}{\partial t} + T] - \frac{2h}{t_p} (T - T_a) - \tau_q \frac{2h}{t_p} \frac{\partial}{\partial t} (T - T_a) + \frac{g}{t_p} + \frac{\tau_q}{t_p} \frac{\partial g}{\partial t} \quad (3)$$

Initial and boundary conditions are [8]:

$$T(x,t) = T_a, \text{ for } t = 0 \quad (4)$$

$$\frac{\partial T(x,t)}{\partial t} = 0, \text{ for } t = 0 \quad (5)$$

$$\frac{\partial T(x,t)}{\partial x} = 0, \text{ at } x = 0 \quad (6)$$

$$T(x,t) = T_t, \text{ at } x = L \quad (7)$$

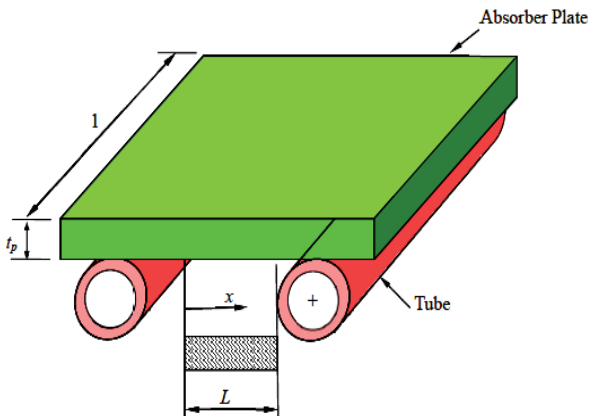


Fig. 1 Schematic of a symmetric heat transfer module in an absorber plate

The following dimensionless variables are introduced:

$$\theta = \frac{T - T_a}{T_t - T_a}, \eta = \frac{x}{L}, \xi = \frac{\alpha t}{L^2}, G = \frac{gL^2}{k(T_t - T_a)t_p}, \beta = L\sqrt{2h/kt_p}, v = \sqrt{\alpha/\tau_q}, V_e = \tau_q v/L \quad (8)$$

where  $V_e$  is the Vernotte number. Based on  $\tau_q$ , the

propagation speed  $v$  is defined in (8). It is also known as the thermal wave speed. Introducing these dimensionless parameters in (8) into (3)–(7) leads to the following dimensionless differential equation of the present problem as:

$$\frac{\partial^2 \theta}{\partial \eta^2} + R_{Tq} V_e^2 \frac{\partial}{\partial \eta} \left( \frac{\partial^2 \theta}{\partial \eta \partial \xi} \right) - \beta^2 \theta - V_e^2 \beta^2 \frac{\partial \theta}{\partial \xi} + G + V_e^2 \frac{\partial G}{\partial \xi} = \frac{\partial \theta}{\partial \xi} + V_e^2 \frac{\partial^2 \theta}{\partial \xi^2} \quad (9)$$

subjected to the dimensionless boundary and initial conditions:

$$\frac{\partial \theta(\eta, \xi)}{\partial \eta} = 0, \text{ at } \eta = 0 \quad (10)$$

$$\theta(\eta, \xi) = 1, \text{ at } \eta = 1 \quad (11)$$

$$\theta(\eta, \xi) = 0, \text{ for } \xi = 0 \quad (12)$$

$$\frac{\partial \theta(\eta, \xi)}{\partial \xi} = 0, \text{ for } \xi = 0 \quad (13)$$

where  $R_{Tq} = \tau_T / \tau_q$

#### B. Numerical Analysis

The method of the Laplace transform is employed to remove the time-dependent terms from (9)–(11) with the initial conditions (12) and (13). The Laplace transforms of (9)–(11) give:

$$\frac{d^2 \bar{\theta}}{d\eta^2} - \lambda^2 \bar{\theta} = R \quad (14)$$

$$\frac{d\bar{\theta}(\eta, s)}{d\eta} = 0, \text{ at } \eta = 0 \quad (15)$$

$$\bar{\theta}(\eta, s) = 1/s, \text{ at } \eta = 1 \quad (16)$$

where,

$$\lambda^2 = \frac{(s + \beta^2)(s \cdot V_e^2 + 1)}{(s \cdot R_{Tq} V_e^2 + 1)}, R = \frac{-[G + \int_0^\infty V_e^2 \frac{\partial G}{\partial \xi} e^{-s\xi} d\xi]}{(s \cdot R_{Tq} V_e^2 + 1)} \quad (17)$$

Subsequently, (14) can be discretized by using a control volume formulation. Integration of (14) within a small control volume  $[\eta_i - l/2, \eta_i + l/2]$  for the  $i$ th interior node can be written as [10]:

$$\int_{\eta_i - l/2}^{\eta_i + l/2} \left[ \frac{d^2 \bar{\theta}}{d\eta^2} - \lambda^2 \bar{\theta} - R \right] d\eta = 0 \quad (18)$$

where  $l$  is the distances between two neighboring nodes.

As illustrated by Liu and Wang [6],  $\bar{\theta}$  in (18) can be approximated by using the nodal temperatures and shape functions within a small control volume before performing the integration of (18). Liu et al. [11] stated that the selection of the shape functions is an important step in order to obtain more accurate numerical results of the problem. A poor selection of the shape functions will affect the accuracy and stability of the numerical results. It can be found from the previous works that the hyperbolic shape functions derived from the associated differential equation in the transform domain can be successfully applied to suppress numerical oscillations in the vicinity of the jump discontinuity [5], [12]. Thus, the shape functions in the present study will be derived from the following associated homogeneous differential equation:

$$\frac{d^2 \bar{\theta}}{d\eta^2} - \lambda^2 \bar{\theta} = 0, \text{ for } \eta_i \leq \eta \leq \eta_{i+1}, i = 1, 2, \dots, N-1 \quad (19)$$

The following simple notations will be also used:

$$\bar{\theta}(\eta_i) = \bar{\theta}_i \text{ and } \bar{\theta}(\eta_{i+1}) = \bar{\theta}_{i+1} \quad (20)$$

The general solution of (19) in the interval  $[\eta_i, \eta_{i+1}]$  with the boundary conditions shown in (20) is:

$$\bar{\theta}(\eta) = \frac{1}{\sinh(\lambda l)} [\sinh(\lambda(\eta_i + l - \eta)) \bar{\theta}_i + \sinh(\lambda(\eta - \eta_i)) \bar{\theta}_{i+1}] \quad (21)$$

Similarly, the analytical solution of (19) in the interval  $[\eta_{i-1}, \eta_i]$  is:

$$\bar{\theta}(\eta) = \frac{1}{\sinh(\lambda l)} [\sinh(\lambda(\eta_i - \eta)) \bar{\theta}_{i-1} + \sinh(\lambda(\eta - \eta_i + l)) \bar{\theta}_i] \quad (22)$$

It is evident that (18) can be rewritten as:

$$\left. \frac{d\bar{\theta}}{d\eta} \right|_{\eta_i+l/2} - \left. \frac{d\bar{\theta}}{d\eta} \right|_{\eta_i-l/2} - \lambda^2 \int_{\eta_i-l/2}^{\eta_i+l/2} \bar{\theta} d\eta = \int_{\eta_i-l/2}^{\eta_i+l/2} R d\eta \quad (23)$$

Inserting the approximations for  $\bar{\theta}$ , (21) and (22), and then evaluating the resulting integrals can produce the following discretized form for the interior nodes as:

$$B_{i-1} \bar{\theta}_{i-1} + B_i \bar{\theta}_i + B_{i+1} \bar{\theta}_{i+1} = F_i, \text{ for } i = 2, 3, \dots, N-1 \quad (24)$$

The coefficients  $B_{i-1}$ ,  $B_i$ ,  $B_{i+1}$ , and  $F_i$  are given as:

$$B_{i-1} = B_{i+1} = 1, B_i = -2 \cosh(\lambda l), F_i = R l \sinh(\lambda l) / \lambda \quad (25)$$

Rearrangement of (24) in conjunction with the discretized forms of the boundary conditions yields the following matrix equation:

$$[B] \{ \bar{\theta} \} = \{ F \} \quad (26)$$

where  $[B]$  is a matrix with complex numbers,  $\{ \bar{\theta} \}$  is a column vector representing the unknown dimensionless nodal temperatures in the Laplace transform domain, and  $\{ F \}$  is a column vector representing the forcing term. Thereafter, the numerical inversion formula, known as the Fourier series technique [13], can be applied to yield the nodal temperatures  $\{ \theta \}$  in the physical domain.

### III. RESULTS AND DISCUSSION

The purpose of the present work is to numerically study the thermal behavior in the absorber plates of a flat-plate solar collector based on the DPL heat conduction model. In the following computations, the distance between two nodes  $l = 0.005$  is applied. For the illustration of numerical analysis, the present study assumes that the solar energy is incident on the plate with a constant rate of  $G = 1$ , although it can be any function in the above analysis [8].

Fig. 2 depicts the temperature distributions in the absorber plate at various times with  $\tau_r / \tau_q = 0.1$ ,  $V_e = 0.2$ ,  $G = 1$ , and  $\beta = 0.5$  for a constant temperature  $\theta = 1$  at  $\eta = 1$ . These results are obtained while maintaining an isothermal condition of the plate at the boundary  $\eta = 1$ . The curves with  $\tau_r = 0$  correspond to the thermal wave solutions. With the thermal wave model, it can be found in Fig. 2 that the temperature near interior boundary  $\eta = 0$  is undisturbed during the initial stage of heating before jumping instantaneously. This may be viewed as the wave-front emerging from the finite propagation of the thermal wave or the existence of the relaxation time  $\tau_q$ . The transmitted wave in the absorber plate at  $\xi = 0.22$  has impacted the interior boundary  $\eta = 0$  and reflected. The results from the DPL model exhibit dissimilar behavior and differ from the results of thermal wave model. Unlike thermal wave model, no wave behavior is observed in the DPL model as expected, but a non-Fourier diffusion-like behavior exists due to the second thermal relaxation time  $\tau_r$  whose effect is to weaken the thermal wave, thereby destroying the sharp wave-front.

Fig. 3 illustrates the effect of the design parameter  $\beta$  on the temperature response in the absorber plate. The results in Fig. 3 are obtained at  $\xi = 0.15$  with  $\tau_r / \tau_q = 0.1$ ,  $V_e = 0.2$ , and  $G = 1$  for a constant temperature  $\theta = 1$  at  $\eta = 1$ . The parameter  $\beta$  decreases the magnitude of the temperature response by increasing the thermal resistance. However, the nature of the response is unaltered. In addition, the variation of parameter  $\beta$  has no effect on the propagation speed  $v$  of the thermal wave, which can be expected from the definition of  $v$ .

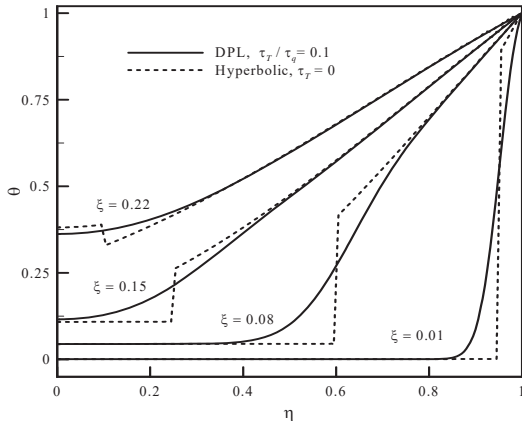


Fig. 2 Temperature distributions in the absorber plate at various times with  $\tau_T/\tau_q = 0.1$ ,  $V_e = 0.2$ ,  $G = 1$ , and  $\beta = 0.5$

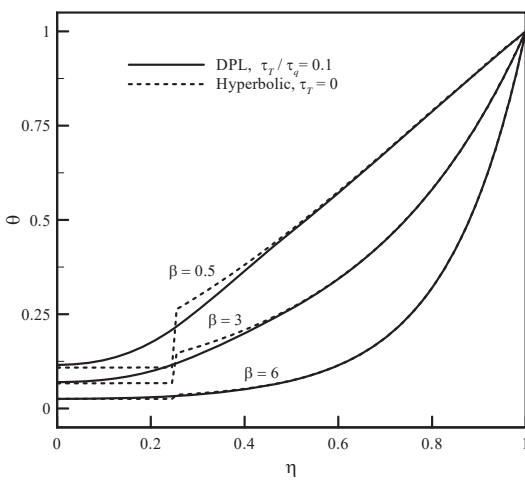


Fig. 3 Temperature distributions in the absorber plate at  $\xi = 0.15$  with  $\tau_T/\tau_q = 0.1$ ,  $V_e = 0.2$ , and  $G = 1$

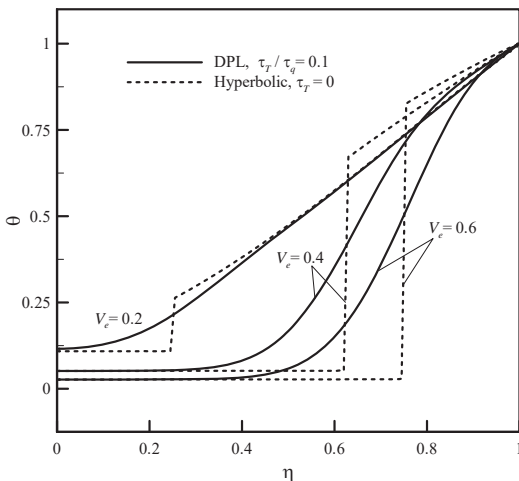


Fig. 4 Temperature distributions in the absorber plate at  $\xi = 0.15$  with  $\tau_T/\tau_q = 0.1$ ,  $G = 1$ , and  $\beta = 0.5$

The temperature distributions for various values of Vernotte number  $V_e$  at  $\xi = 0.15$  are shown in Fig. 4 with  $\tau_T/\tau_q = 0.1$ ,  $G = 1$ , and  $\beta = 0.5$  for an isothermal boundary temperature  $\theta = 1$  at  $\eta = 1$ . It can be found that the thermal wave travels with a longer distance for a smaller value of  $V_e$ . This phenomenon can be explained by observing the definitions of the Vernotte number and the propagation speed  $v$  of the thermal wave as shown in (8), which states that a smaller value of the Vernotte number  $V_e$  implies a smaller relaxation time  $\tau_q$  and thus a faster propagation speed of the thermal wave. In addition, the sharp wave-fronts are smoothed and the portions of pulse thermal disturbances are dissipated by the diffusive effect of  $\tau_T$ .

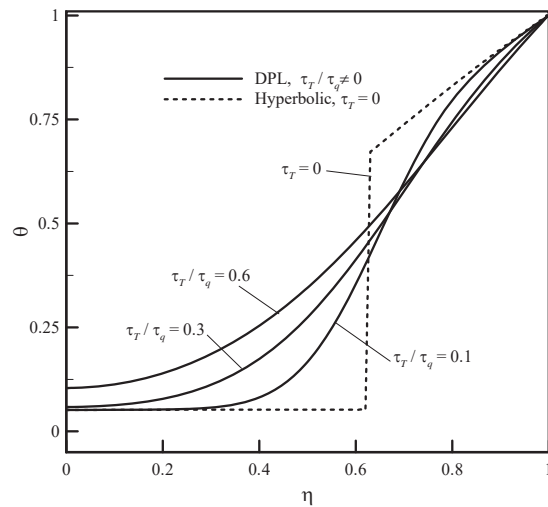


Fig. 5 Temperature distributions in the absorber plate at  $\xi = 0.15$  with  $V_e = 0.4$ ,  $G = 1$ , and  $\beta = 0.5$

Fig. 5 demonstrates the effect of ratio  $\tau_T/\tau_q$  on the temperature profile in the absorber plate. Those results in Fig. 5 are calculated at  $\xi = 0.15$  with  $V_e = 0.4$ ,  $\beta = 0.5$ , and  $G = 1$  for a constant temperature  $\theta = 1$  at  $\eta = 1$ . As can be seen from Fig. 5, for the hyperbolic case ( $\tau_T = 0$ ), the delay of  $\tau_q$  induces a thermal wave with sharp wave-front separating heated and unheated zones in the absorber plate. Nevertheless, no obvious wave-fronts can be found for the DPL cases, which are attributable to the stronger dissipation from the mixed derivative term ( $k\tau_T\partial^2/\partial x^2(\partial T/\partial t)$ ), as shown in (3). The results are almost the same for all different values of  $\tau_T/\tau_q$  ratio. The sharp wave-fronts due to  $\tau_q$  are smoothed by the promoting conduction of  $\tau_T$ , and the effect is more noticeable with increasing values of  $\tau_T/\tau_q$  ratio, leading to the non-Fourier diffusion-like conduction [14].

## ACKNOWLEDGMENT

This work was supported by the Ministry of Science and Technology, Taiwan, Republic of China, under the grant number MOST 104-2221-E-168-020.

## REFERENCES

- [1] B. Kundu, "Performance and optimum design analysis of an absorber plate fin using recto-trapezoidal profile," *Solar Energy*, vol. 62, pp. 22–32, 2008.
- [2] D.-Y. Tzou, "A unified field approach for heat conduction from macro- to micro-scales," *ASME J. Heat Transfer*, vol. 117, pp. 8–16, 1995.
- [3] D.-Y. Tzou, "Experimental support for the lagging response in heat propagation," *AIAA J. Thermophys. Heat Transfer*, vol. 9, pp. 686–693, 1995.
- [4] K.-Q. Hu and Z.-T. Chen, "Transient heat conduction analysis of a cracked half-plane using dual-phase-lag theory," *Int. J. Heat Mass Transfer*, vol. 62, pp. 445–451, 2013.
- [5] H.-L. Lee, W.-L. Chen, W.-J. Chang, E.-J. Wei, and Y.-C. Yang, "Analysis of dual-phase-lag heat conduction in short-pulse laser heating of metals with a hybrid method," *Appl. Therm. Eng.*, vol. 52, pp. 275–283, 2013.
- [6] K.-C. Liu and J.-C. Wang, "Analysis of thermal damage to laser irradiated tissue based on the dual-phase-lag model," *Int. J. Heat Mass Transfer*, vol. 70, pp. 621–628, 2014.
- [7] N. Afrin, Y. Zhang, J.-K. Chen, "Dual-phase lag behavior of a gas-saturated porous-medium heated by a short-pulsed laser," *Int. J. Therm. Sciences*, vol. 75, pp. 1–27, 2014.
- [8] B. Kundu, K.-S. Lee, "Fourier and non-Fourier heat conduction analysis in the absorber plates of a flat-plate solar collector," *Solar Energy*, vol. 86, pp. 3030–3039, 2012.
- [9] R. T. Al-Khairi, "Analytical solution of the hyperbolic heat conduction equation for a moving finite medium under the effect of time dependent laser heat source," *ASME J. Heat Transfer*, vol. 134, pp. 122402-1–122402-7, 2012.
- [10] H.-L. Lee, T.-H. Lai, W.-L. Chen, and Y.-C. Yang, "An inverse hyperbolic heat conduction problem in estimating surface heat flux of a living skin tissue," *Appl. Math. Model.*, vol. 37, no. 5, pp. 2630–2643, 2013.
- [11] K.-C. Liu, Y.-N. Wang, and Y.-S. Chen, "Investigation on the bio-heat transfer with the dual-phase-lag effect," *Int. J. Therm. Sciences*, vol. 58, pp. 29–35, 2012.
- [12] H.-L. Lee, W.-L. Chen, W.-J. Chang, and Y.-C. Yang, "Estimation of energy absorption rate and temperature distributions in short-pulse laser heating of metals with a dual-phase-lag model," *Appl. Therm. Eng.*, vol. 65, no. 1–2, pp. 352–360, 2014.
- [13] Y.-C. Yang, H.-L. Lee, J.-C. Hsu, and S.-S. Chu, "Thermal stresses in multilayer gun barrel with interlayer thermal contact resistance," *J. Therm. Stresses*, vol. 31, pp. 624–637, 2008.
- [14] T.-S. Wu, H.-L. Lee, W.-J. Chang, and Y.-C. Yang, "An inverse hyperbolic heat conduction problem in estimating pulse heat flux with a dual-phase-lag model," *Int. Comm. Heat Mass Transfer*, vol. 60, pp. 1–8, 2015.